

criterion defines "elastic scattering" for this experiment. By varying the electron energy in the betatron and at the same time the discriminator bias, it is possible to observe the scattering as a function of photon energy. Figure 1 shows the experimental

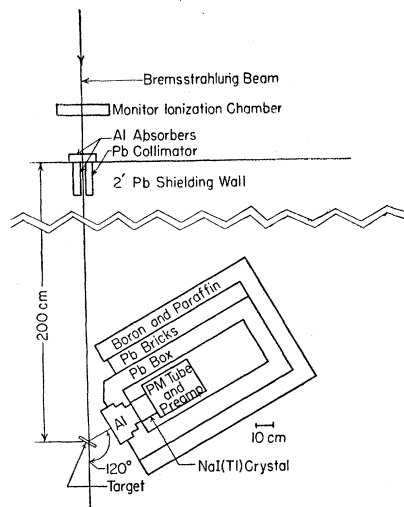


FIG. 1. Experimental arrangement. The counter and associated shielding is mounted on a table that rotates about a pivot below the target.

arrangement. The aluminum absorbers harden both the direct and scattered beams in order to decrease the number of small pulses contributing to pileup.

The experimental procedure is to observe the number of counts ( $N_1$ ) produced for a charge ( $Q_1$ ) collected on the ionization chamber when the crystal is in the direct beam from the betatron at the zero degree position. These counts are detected in the differential channel positioned just below the tip of the pulse-height distribution produced by the filtered bremsstrahlung spectrum. The crystal is then swung to the  $120^\circ$  position, and the number of counts ( $N_2$ ) for a charge ( $Q_2$ ) collected on the ionization chamber is determined. The differential cross section is given by:

$$\frac{d\sigma}{d\Omega_{120}} = C \frac{Q_1}{N_1} \times \frac{N_2}{Q_2} \text{ mb/sterad,}$$

where the constant  $C$  contains geometrical factors, the number of atoms of the target irradiated, and a correction for absorption in the target. The maximum counting rates in the scattered beam are about 20 per hour,  $Q_1/Q_2 \sim 10^{-5}$ . Cosmic-ray background in the differential channel is less than one count per hour. The data are corrected for this background and for neutron background from the uranium target.

The results are given in Table I. The energy spreads indicated are determined from the width of the discriminator channel and the errors indicated for the intensities are the standard deviations based only on the numbers of counts. Systematic errors, while not affecting the relative values, may be large enough to make the absolute cross section in error by as much as twenty-five percent.

The lead data are plotted in Fig. 2. The absolute cross section at 17 Mev agrees with the value obtained by Stearns.<sup>3</sup> The "resonance" scattering by Pb and Au peaks near 15 Mev and at a

TABLE I. Elastic scattering cross sections in mb/sterad.

$E$ (Mev)	Au	Pb	U
9.00-9.75	$0.08 \pm 0.03$	$0.19 \pm 0.06$	$0.16 \pm 0.04$
11.3-12.3	$0.20 \pm 0.04$	$0.24 \pm 0.05$	$0.45 \pm 0.08$
14.0-15.1	$0.60 \pm 0.10$	$0.81 \pm 0.11$	$0.59 \pm 0.12$
15.2-16.3	$0.58 \pm 0.10$	$0.77 \pm 0.13$	$0.49 \pm 0.12$
17.6-19.6	$0.32 \pm 0.06$	$0.37 \pm 0.08$	$0.20 \pm 0.07$
21.7-24.3	$0.11 \pm 0.04$	$0.23 \pm 0.06$	$0.18 \pm 0.06$

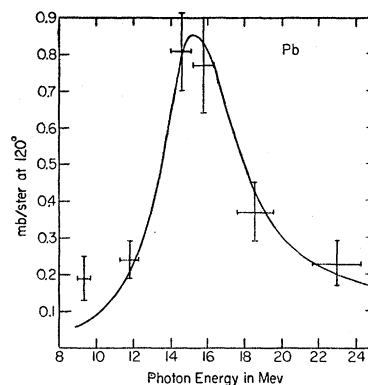


FIG. 2. The elastic scattering cross section for lead. The indicated spread in energy is the width of the differential discriminator channel, and the standard deviations are based only on the number of counts. The smooth curve is a Breit-Wigner single resonance curve normalized to give a cross section of 0.85 mb/sterad at 15 Mev ( $\hbar\omega_0 = 15$  Mev,  $\Gamma = 5$  Mev).

slightly lower energy for U. The "resonances" are about 5 Mev wide for all three elements. Further experiments are underway extending these measurements both to lighter materials and over a greater energy range.

The authors would like to thank Dr. U. Fano and Dr. H. W. Koch for their interest.

\* This research was supported by the U. S. Air Force, through the Office of Scientific Research of the Air Research and Development Command.

<sup>1</sup> M. Goldhaber and E. Teller, Phys. Rev. **74**, 1046 (1948); H. Steinwedel and J. H. D. Jensen, Z. Naturforsch. **5a**, 413 (1950); J. Levinger and H. Bethe, Phys. Rev. **78**, 115 (1950); Ferntz, Gell-Mann, and Pines, Phys. Rev. **92**, 836 (1953); A. Reifmann, Z. Naturforsch. **8a**, 505 (1953).

<sup>2</sup> E. R. Gaertner and M. L. Yeater, Phys. Rev. **76**, 363 (1949); Dressel, Goldhaber, and Hanson, Phys. Rev. **77**, 754 (1950); M. B. Stearns, Phys. Rev. **87**, 706 (1952).

<sup>3</sup> R. S. Foote and H. W. Koch, Rev. Sci. Instr. (to be published).

## Angular Anisotropy of Specific Thorium Photofission Fragments\*

A. W. FAIRHALL, I. HALPERN,<sup>†</sup> AND E. J. WINHOLD

Laboratory for Nuclear Science, Massachusetts Institute of Technology, Cambridge, Massachusetts

(Received March 8, 1954)

ANISOTROPY in the angular distribution of photofission fragments from thorium has previously been observed by counting the total  $\beta$  activity of the fragments caught at various angles with respect to the x-ray beam.<sup>1</sup> The present measurements, which were also performed using 16-Mev thick-target bremsstrahlung<sup>†</sup> from the MIT linear accelerator, compare the number of fragments emitted per unit solid angle at  $90^\circ$  to the x-ray beam to the average of the numbers at  $0^\circ$  and  $180^\circ$  for seven specific fission-product elements: bromine, silver, antimony, tellurium, iodine, barium, and cerium. Over the range measured, the anisotropy appears to be a monotonically increasing function of the mass ratio of the fission fragment pairs.

The collimated fragments were caught in thin foils, specific fission elements were separated with carriers, and their respective  $\beta$  activities measured and corrected for chemical yield and radioactive decay. The exposure arrangement consisted of a series of thorium and catcher foils alternated and separated by aluminum collimators, as shown in Fig. 1. Two such stacks were mounted on the periphery of a turntable and were rotated alternately into the beam for five-minute intervals during each four-hour exposure. When in the beam one stack had its axis parallel, the other its axis perpendicular to the x-ray beam. Using thin aluminum catchers, the  $\beta$  activity of the unseparated fragments was first measured, after which barium and tellurium were radio-chemically separated and counted. To facilitate the chemical separations of the other elements, thin films of ice were substituted for the aluminum foils, and barium was separated in every run as an internal standard.

At least six measurements were made on all the elements except antimony, which was measured four times.

For 85-min  $Ba^{139}$ , the ratio of the  $90^\circ$  activity to the  $(0^\circ+180^\circ)$  activity was found to be the same (within 1 percent) as the corresponding ratio for unseparated fission product  $\beta$  activity. The  $90^\circ/(0^\circ+180^\circ)$  ratios for the other elements were all measured in terms of the ratio for barium, which was separated in all runs. The

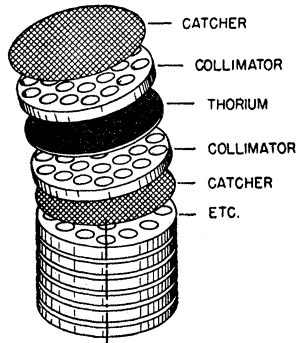


FIG. 1. An exploded view of one of the two stacks of foils and collimators. The axis of the stack is oriented either parallel or perpendicular to the x-ray beam. The half-angle of the collimator holes is  $15^\circ$ .

angular distribution of the unseparated fragments has been measured previously<sup>1</sup> using the same bremsstrahlung beam, and was found to be compatible with the form  $a+b \sin^2\theta$  with respect to the x-ray beam. The experimental value of  $b/a$  was found to be  $0.41 \pm 0.05$ . The values of  $b/a$  for the other elements, taking barium

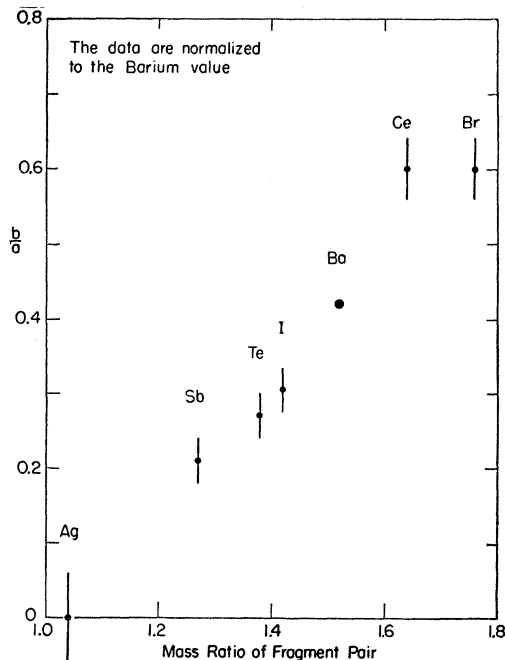


FIG. 2. Angular anisotropy of  $Th^{232}$  fission fragments as a function of the mass ratio of the fragment pair.

to be 0.41 exactly, are shown in Fig. 2, plotted as a function of the mass ratio of heavy-to-light fission fragment pair.

The errors shown on the points are probable errors based on the spread of the values obtained in the different runs. The experimental procedure was checked for systematic errors by making several runs with only one stack, dividing the catchers in two equal portions and separating several elements in each portion. The ratios of the fission yields of the several elements were the same within 5 percent in each of the two portions, indicating that

the errors of chemical separation, determination of chemical yield, and counting are small.

The data of Fig. 2 imply that the mass-yield curve for the  $\sin^2\theta$  component of the angular distribution is warped toward greater mass asymmetry than the curve for the isotropic component. But whatever the mechanism leading to the angular anisotropy, both curves display the same sort of double-humped shape characteristic of various types of fission, including photofission,<sup>2-4</sup> in this general energy region.

We hope, with increased beam currents, to repeat the experiment at lower energies where the angular anisotropy is larger.

\* This work was supported in part by the joint program of the U. S. Office of Naval Research and the U. S. Atomic Energy Commission.

† Now at the Department of Physics, University of Washington, Seattle, Washington.

‡ The electron beam used had a maximum energy of 16 Mev and a broad energy spectrum peaked at about 13 Mev, with a width at half-maximum of 5 Mev.

<sup>1</sup> Winhold, Demos, and Halpern, Phys. Rev. **87**, 1139 (1952).

<sup>2</sup> R. A. Schmitt and N. Sugarman, Phys. Rev. **89**, 1155 (1953).

<sup>3</sup> H. G. Richter and C. D. Coryell, Phys. Rev. **90**, 389 (1953).

<sup>4</sup> D. M. Hiller and D. S. Martin, Jr., Phys. Rev. **90**, 581 (1953).

## Decay Scheme of $Xe^{135}$

SIGVARD THULIN

Nobel Institute of Physics, Stockholm, Sweden

(Received March 16, 1954)

THE 9.2-hr  $Xe^{135}$  has been shown to decay by emission of 910-keV  $\beta$  particles to an excited level of energy 250 keV in  $Cs^{135}$ .<sup>1,2</sup> Moreover, a very weak  $\gamma$  ray of energy 610 keV has been reported.<sup>2</sup> This  $\gamma$  ray has now been studied by means of coincidence measurements on electromagnetically separated  $Xe^{135}$  samples in an intermediate image  $\beta$  spectrometer.<sup>3</sup> Behind the  $\beta$  source a large NaI(Tl) crystal (diameter 1 in.  $\times$  1 in.) was placed. This was optically connected with an EMI 6262 photomultiplier by means of a perspex light pipe of 15-cm length. The G-M pulses and the scintillation spectrometer pulses were fed to a coincidence circuit of resolving time  $2.5 \times 10^{-7}$  sec.

No coincidences were found between  $K$  conversion electrons of the 250-keV  $\gamma$  ray and  $\gamma$  quanta of energy higher than 550 keV. However, coincidences were recorded between these  $K$ -conversion electrons and  $\gamma$  quanta of energy  $\sim 370$  keV. A small bump on the high-energy tail of the very strong 250-keV  $\gamma$  line in the scintillation spectrum of  $Xe^{135}$  may partly be explained as due to a  $\gamma$  ray of energy  $\sim 370$  keV.

It was also shown that the 600-keV  $\gamma$  ray is emitted in cascade with a  $\beta$  continuum. A Fermi plot of the coincidence distribution showed an upper limit of 548 keV.

The results of the coincidence measurements strongly support the decay scheme given in Fig. 1.

According to the extreme one-particle shell model,<sup>4</sup> the second excited level might be  $s_{3/2}$  or  $d_{3/2}$ . The former alternative seems im-

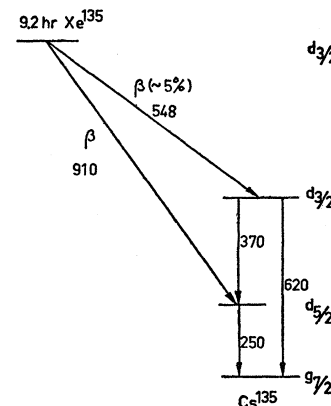


FIG. 1. Proposed decay scheme of  $Xe^{135}$ . Energy values in keV.